

Phase driven exact and unconventional superradiance phase transition in non-Hermitian cascaded Rabi cavities

Shujie Cheng,^{1,2} Shuai-Peng Wang,^{3,4} G. D. M. Neto,² and Gao Xianlong²

¹*Xingzhi College, Zhejiang Normal University, Lanxi 321100, China*

²*Department of Physics, Zhejiang Normal University, Jinhua 321004, China*

³*Quantum Physics and Quantum Information Division,*

Beijing Computational Science Research Center, Beijing 100193, China

⁴*Zhejiang Province Key Laboratory of Quantum Technology and Device, School of Physics, and State Key Laboratory for Extreme Photonics and Instrumentation, Zhejiang University, Hangzhou 310027, China*

(Dated: June 25, 2024)

This work reports the phase driven symmetry breaking and exact and unconventional superradiance phase transition in the non-Hermitian cascaded Rabi cavities. The non-Hermiticity is introduced in the coupling phase (denoted by φ) between the atom and the optical field. The exactness refers to the fact that the superradiance phase boundary is obtained analytically and verified by the observables. The unconventionality is reflected in that when $|\varphi| = \frac{\pi}{4}$ or $|\varphi| = \frac{3\pi}{4}$, the phase boundary is uniquely determined by $\mathcal{J} = \frac{1}{2}$ (where \mathcal{J} is the dimensionless cavity coupling strength) and is independent of the atom-optical field coupling strength g . For other φ , the phase boundary is determined by \mathcal{J} and the dimensionless atom-optical field coupling strength g together. Besides, we find that there are phase driven first-order and second-order superradiance phase transitions, and the quantum criticality for the second-order superradiance phase transition is studied. In addition, the experimental feasibility is discussed. This work will stimulate the studies of non-Hermitian superradiance quantum phase transitions and their experimental realizations, as well as the underlying universality class of phase transitions.

PACS numbers: 64.60.-i, 05.70.Fh, 64.60.Fr

I. INTRODUCTION

The quantum Rabi model (QRM) named as Rabi [1, 2] describes the interaction of a two-level atom and a single-model optical field and can be viewed as the minimal version of the Dicke model [3]. In the past years, there are efforts in finding the exactly analytically solutions of the QRM [4–11]. Employing the Bargmann space representation [12], Braak obtained the transcendental function, namely the G-function, and found that the poles of the G-function were the exact solutions of QRM [13]. Quickly, Chen et al. obtained the exact solutions of a two-photon QRM by combining the Bogoliubov transformation and the G-function [14]. In the decade, the two methods have been used for calculating the exact solutions of the generalized QRMs [15–25]. It was found that the symmetry breaking will lead to the topological transition in the QRM [26] and the generalized QRM [27].

Accompanying by the search for the exact solutions, there are interests in studying the quantum criticality of the QRMs or the generalized QRMs [28–36]. Accompanied by the quantum phase transition, i.e., the superradiance phase transition (SPT), there will occur macroscopic photon excitations [31]. In 2015, Hwang et al. studied the universal dynamics and the critical behaviors of the QRM and the exact phase boundary of SPT was obtained by an effective low-energy approximation [28]. They found that the critical exponent of SPT ν is $\nu = \frac{3}{2}$ [28]. By analyzing a general scaling function, Liu et al. found that the ν in the anisotropic QRM still satisfies $\nu = \frac{3}{2}$ and the phase boundary of SPT is ob-

tained by a semi-class method [30]. Quickly, Wei et al. numerically verified the exact ν by analyzing the critical behaviors of the finite frequency fidelity susceptibility [32]. Subsequent researches show that for a multi-cavity system with two [33, 34] or three [36] cascaded QRMs, the critical exponent is still equal to that of a single Rabi model, but for a three-level QRM, there occurs new critical exponent with $\nu = 1$ [37]. We notice that the SPTs in the QRMs more or less depend on the atom-optical field coupling strength. It motivate us whether there exist an unconventional SPT which is independent of the atom-optical field coupling.

Recently, the combination of the non-Hermiticity and the QRMs triggered intriguing physics. Cao et al. constructed a generalized non-Hermitian integrable QRM. They obtained the exact energy spectrum and eigenstates of this model by employing the Bethe ansatz [38]. The work provides a generalized strategy to engineer integrable non-Hermitian spin-boson models. By introducing the parity-time (\mathcal{PT}) symmetric gain and loss in the semi-classical Rabi model, Lee et al. [39] found that there was \mathcal{PT} symmetry breaking [40, 41] accompanied by the real-complex transition in energy. With the exact solutions of the \mathcal{PT} -symmetric Rabi models, one can locate the \mathcal{PT} -symmetry breaking point, i.e., the exceptional point (EP) [42]. Xie et al. investigated the Floquet \mathcal{PT} -symmetric semi-classical Rabi model [43]. Under the multiple-photon resonance condition, they obtained the positions of the EPs from the exact Floquet spectrum. Employing the adiabatic approximation, Lu et al. obtained the exact energy spectrum of the \mathcal{PT} -

symmetric QRM, by which the EPs were located [44]. With the emergence of EP, observables present discontinuous behaviors. By the Bogoliubov transformation and G-function, Li et al. solved the exact energy spectra for a one-photon and two-photon \mathcal{PT} -symmetric QRM, and the zeros of G-function located the EPs [45]. These works provide an inspiration for us to study whether there will be a completely real energy spectrum in a generalized non-Hermitian QRM without \mathcal{PT} symmetry. In addition, we will study the quantum criticality of the model and discuss the similarity and difference with Hermitian cases.

The paper is organized as follows. In Sec. II we introduce the generalized non-Hermitian QRM without \mathcal{PT} symmetry. In Sec. III, we obtain the exact phase boundary of the model. In Sec. IV, we study the observables which signal the SPT. In Sec. V, we discuss the quantum criticality of the SPT. An experimental feasibility is discussed in Sec. VI, and a summary is presented in Sec. VII.

II. TWO COUPLED NON-HERMITIAN RABI CAVITIES

The generalized non-Hermitian QRM without \mathcal{PT} symmetry is constructed by two cascaded non-Hermitian Rabi cavities, whose Hamiltonian ($\hbar = 1$) is given as

$$H = \sum_{j=1,2} h_j + J(a_1^\dagger + a_1)(a_2^\dagger + a_2), \quad (1)$$

where h_j describes non-Hermitian Rabi cavity $h_j = \omega_p a_j^\dagger a_j + \frac{\omega_a}{2} \sigma_z^j - \lambda e^{i\varphi} (a_j + a_j^\dagger) \sigma_x^j$ with j the cavity index and a_j^\dagger (a_j) the creation (annihilation) of photons. ω_p is the optical field frequency, ω_a is the atomic frequency, and $\lambda e^{i\varphi}$ is the coupling strength between the atom and optical field with λ the weight of strength and φ the coupling phase. The non-Hermiticity of the system requires $\varphi \in (-\pi, 0) \cup (0, \pi)$.

For a single non-Hermitian Rabi cavity, we argue that there is no parity-time (\mathcal{PT}) symmetry unless the coupling phase $\varphi = \pm \frac{\pi}{2}$. The time-reversal operator \mathcal{T} dominates the complex conjugate operation, resulting in $\mathcal{T} a_j^\dagger (a_j) \mathcal{T} = a_j^\dagger (a_j)$. The parity operator \mathcal{P} dominates the inversion operation, i.e., $\mathcal{P} \hat{x}_j \mathcal{P} = -\hat{x}_j$, and $\mathcal{P} \hat{p}_j \mathcal{P} = -\hat{p}_j$ [40]. Thus, we have

$$\begin{aligned} \mathcal{PT} h_j \mathcal{PT} &= \omega_p a_j^\dagger a_j - \mathcal{P} \left[\lambda e^{-i\varphi} (a_j + a_j^\dagger) \sigma_x^j \right] \mathcal{P} + \frac{\omega_a}{2} \sigma_z^j \\ &= \omega_p a_j^\dagger a_j + \lambda e^{-i\varphi} (a_j + a_j^\dagger) \sigma_x^j + \frac{\omega_a}{2} \sigma_z^j. \end{aligned} \quad (2)$$

Only if $\varphi = \pm \frac{\pi}{2}$, the single non-Hermitian Rabi cavity is \mathcal{PT} -symmetric (see another prove in Ref. [45]). For other values, it is not \mathcal{PT} -symmetric.

For the cascaded non-Hermitian QRM, we demonstrate that this system is completely not \mathcal{PT} -symmetric. \mathcal{P} dominates a mirror operation between the two cavities, i.e., $\mathcal{P} a_j^\dagger (a_j) \mathcal{P} = a_{j'}^\dagger (a_{j'})$, $\mathcal{P} \sigma_z^j (\sigma_x^j) \mathcal{P} = \sigma_z^{j'} (\sigma_x^{j'})$

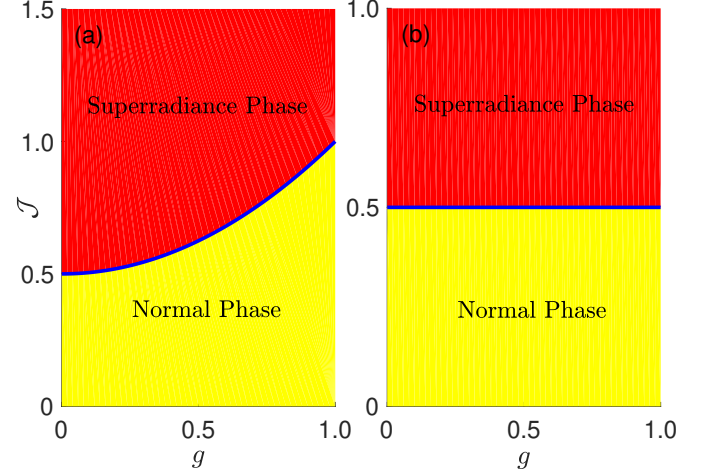


Figure 1. (Color online) Ground-state phase diagram in the J - g parameter space. (a) $\varphi = \frac{\pi}{2}$. (b) $\varphi = \frac{\pi}{4}$. The blue solid lines denote the phase boundary, satisfying $1 - g^2 (\cos^2 \varphi - \sin^2 \varphi) = 2J$.

(here $j \neq j'$), and \mathcal{T} leads to $\mathcal{T}i\mathcal{T} = -i$. Performing \mathcal{PT} on the cavity coupling term, we have

$$\mathcal{PT} J (a_1^\dagger + a_1) (a_2^\dagger + a_2) \mathcal{TP} = J (a_1^\dagger + a_1) (a_2^\dagger + a_2). \quad (3)$$

Performing \mathcal{PT} on h_j , we have

$$\begin{aligned} \mathcal{PT} h_j \mathcal{TP} &= \omega_p a_{j'}^\dagger a_{j'} - \lambda e^{-i\varphi} (a_{j'} + a_{j'}^\dagger) \sigma_x^{j'} + \frac{\omega_a}{2} \sigma_z^{j'} \\ &\neq h_{j'}. \end{aligned} \quad (4)$$

Therefore, here the non-Hermitian cascaded QRM is not \mathcal{PT} -symmetric.

III. EXACT AND UNCONVENTIONAL SUPERRADIANCE PHASE TRANSITION

To analytically solve the phase boundary of the ground-state superradiance phase transition, we introduce the dimensionless parameters $\eta = \frac{\omega_a}{\omega_p}$, $g = \frac{2\lambda}{\sqrt{\omega_a \omega_p}}$, and $\mathcal{J} = \frac{J}{\omega_p}$. Then, the Hamiltonian in Eq. (1) can be rewritten as

$$\frac{H}{\omega_p} = \sum_{j=1,2} \frac{h_j}{\omega_p} + \mathcal{J} (a_1^\dagger + a_1) (a_2^\dagger + a_2), \quad (5)$$

in which

$$\frac{h_j}{\omega_p} = a_j^\dagger a_j + \frac{\eta}{2} \sigma_z^j - \frac{g\sqrt{\eta}}{2} (a_j + a_j^\dagger) \sigma_x^j. \quad (6)$$

Performing the following transformation

$$\begin{aligned} x_j &= (a_j^\dagger + a_j) / \sqrt{2\eta}, \\ y_j &= i (a_j^\dagger - a_j) \sqrt{\eta/2}, \end{aligned} \quad (7)$$

and dividing both sides of Eq. (5) by η , we obtain

$$\mathcal{H} = \frac{H}{\omega_p \eta} \equiv \frac{1}{2} \sum_{j=1,2} \left(x_j^2 + \frac{y_j^2}{\eta^2} + \sigma_z^j - \sqrt{2g} \sigma_x^j x_j \right) + 2\mathcal{J} x_1 x_2. \quad (8)$$

As studied in Refs. [29, 30], the SPT appears in the under the infinite η limit. Under this condition, we can obtain the analytical phase boundary of SPT. When $\eta \rightarrow \infty$, \mathcal{H} reduces to

$$\mathcal{H} = \frac{1}{2} \sum_{j=1,2} \left[x_j^2 + \sigma_z^j - \sqrt{2g} \sigma_x^j x_j \right] + 2\mathcal{J} x_1 x_2. \quad (9)$$

By diagonalizing \mathcal{H} , we obtain the energies $E_{\pm}(x_1, x_2)$ as

$$E_{\pm}(x_1, x_2) = \frac{1}{2} \sum_{j=1,2} \left(x_j^2 \pm \sqrt{1 + 2g^2 x_j^2} \right) + 2\mathcal{J} x_1 x_2. \quad (10)$$

Performing the Taylor expansion on $E_{\pm}(x_1, x_2)$, and truncating them to the quadratic term $\mathcal{O}(x_j^4)$, the low-energy branch $E_{-}(x_1, x_2)$ (contains the ground-state information) becomes

$$E_{-}(x_1, x_2) = \frac{1}{2} \psi^T \Lambda \psi, \quad (11)$$

in which $\psi = (x_1, x_2)^T$ and

$$\Lambda = \begin{pmatrix} 1 - g^2 e^{i2\varphi} & 2\mathcal{J} \\ 2\mathcal{J} & 1 - g^2 e^{i2\varphi} \end{pmatrix}. \quad (12)$$

Evidently, the matrix Λ consists of the real part $\text{Re}(\Lambda)$ and the pure imaginary part $\text{Im}(\Lambda)$ (which can be considered as the background loss), i.e., $\Lambda = \text{Re}(\Lambda) + \text{Im}(\Lambda)$, with

$$\begin{aligned} \text{Re}(\Lambda) &= [1 - g^2 (\cos^2 \varphi - \sin^2 \varphi)] \sigma_0 + 2\mathcal{J} \sigma_x, \\ \text{Im}(\Lambda) &= -i2g^2 \cos \varphi \sin \varphi \sigma_0. \end{aligned} \quad (13)$$

In fact, the phase boundary of SPT is nothing to do with background loss $\text{Im}(\Lambda)$, but is determined by $\text{Re}(\Lambda)$. After diagonalizing $\text{Re}(\Lambda)$, the eigenvalues ϵ_{\pm} of $\text{Re}(\Lambda)$ is obtained as $\epsilon_{\pm} = 1 - g^2 (\cos^2 \varphi - \sin^2 \varphi) \pm 2\mathcal{J}$. When the low-energy branch in ϵ_{\pm} equals to zero, i.e., $\epsilon_{-} = 0$, we can extract the phase boundary of the superradiance phase transition, and it satisfies $1 - g^2 (\cos^2 \varphi - \sin^2 \varphi) = 2\mathcal{J}$. From the expression of the phase boundary, we can see that there are special phases, i.e., $\varphi = \pm \frac{\pi}{4}$ or $\varphi = \pm \frac{3\pi}{4}$, at which the phase boundary is fixed at $\mathcal{J} = \frac{1}{2}$, and is independent of the atom-optical field coupling parameter g . Such type of SPT independent of atom-optical field coupling is counter-intuitive and has not been reported before, so we name this type of SPT as unconventional SPT. While γ is taken at other values, the phase boundary depends on the g and \mathcal{J} together. Thus, we name this atom-optical field coupling dependent SPT as the conventional SPT. Without loss of generality, in the following, we will study the energy, photon population,

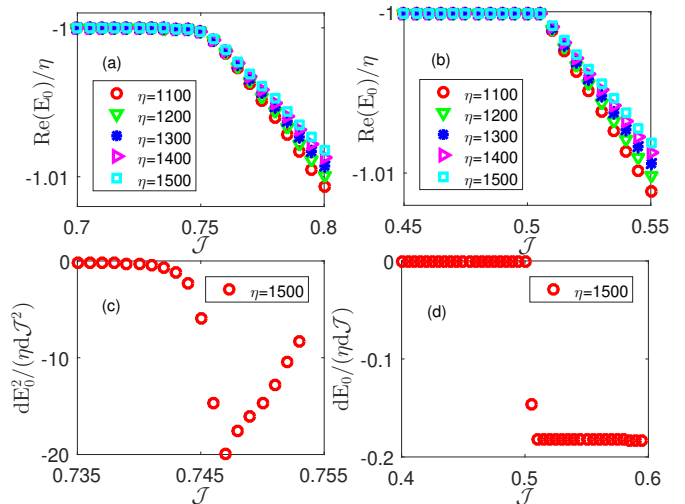


Figure 2. (Color online) The real part of the ground-state energy $\text{Re}(E_0)/\eta$ as a function of \mathcal{J} under different η with $g = 0.7$ and $\phi = \frac{\pi}{2}$ in (a) and with $g = 0.4$ and $\phi = \frac{\pi}{4}$ in (b). (c) The second-order derivative of $\text{Re}(E_0)/\eta$ for $g = 0.7$ and $\phi = \frac{\pi}{2}$. (d) The first-order derivative of $\text{Re}(E_0)/\eta$ for $g = 0.4$ and $\phi = \frac{\pi}{4}$. The photonic truncation number is $N = 80$.

qubit population, the fidelity and the fidelity susceptibility in the ground state at $\varphi = \frac{\pi}{2}$ and $\varphi = \frac{\pi}{4}$ to characterize the properties of the SPT of the non-Hermitian two-Rabi cavity system. The ground state here refers to the state with the smallest real part of the energy. Intuitively, the phase diagrams for $\varphi = \frac{\pi}{2}$ and $\varphi = \frac{\pi}{4}$ are plotted in Fig. 1(a) and 1(b), respectively. The red regions denote the superradiance phases, separated from the normal phases (yellow regions) by the phase boundaries (blues curves).

IV. SIGNATURES OF THE SUPERRADIANCE PHASE TRANSITION

We detect the signatures and check the phase boundary of the SPT. We start by studying the ground-state energy to reveal the SPT. The energies are sorted by the real parts of the energies, and the ground-state energy means the energy with the lowest real part. Under $\varphi = \frac{\pi}{2}$ and different η , the real parts of the ground-state energies $\text{Re}(E_0)/\eta$ as a function of \mathcal{J} for $g = 0.7$ are plotted in Fig. 2(a). The photonic truncation number is taken at $N = 80$. As can be seen that with the emergence of SPT, $\text{Re}(E_0)/\eta$ for different η decrease from -1 to lower values. According to the obtained analytical result, the transition point under $\varphi = \frac{\pi}{2}$ and $g = 0.7$ should be at $\mathcal{J} = 0.745$. Intuitively, the SPT occurs at the transition points predicted by the exactly analytical result (shown with the vertical black line). Meanwhile, we calculate $\text{Re}(E_0)/\eta$ in the $\varphi = \frac{\pi}{4}$ case and $\text{Re}(E_0)/\eta$ - \mathcal{J} relations for $g = 0.4$ are plotted in Fig. 2(b). Similar to the $\varphi = \frac{\pi}{2}$, when \mathcal{J} exceeds to the transition point,

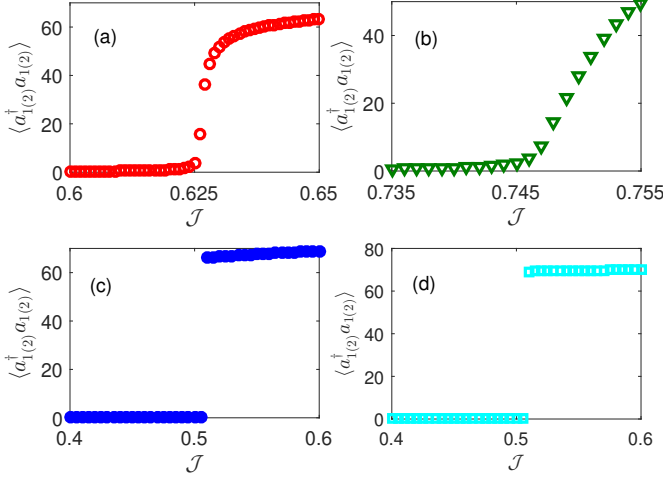


Figure 3. (Color online) The ground-state photon population $\langle a_{1(2)}^\dagger a_{1(2)} \rangle$ as a function of \mathcal{J} . (a) $g = 0.5$ and $\phi = \frac{\pi}{2}$; (b) $g = 0.7$ and $\phi = \frac{\pi}{2}$; (c) $g = 0.4$ and $\phi = \frac{\pi}{4}$; (d) $g = 0.6$ and $\phi = \frac{\pi}{4}$. The photonic truncation number is $N = 80$ and $\eta = 1500$.

$\text{Re}(E_0)/\eta$ for different η in the $\phi = \frac{\pi}{4}$ case decrease from -1 to lower values, signaling the appearance of SPT as well. From the analytical expression of phase boundary, it is known that the transition point under $\phi = \frac{\pi}{2}$ should be at $J = 0.5$ regardless of what value of g is. It is readily seen that for $g = 0.4$, the transition points of $\text{Re}(E_0)/\eta$ occur at the analytically obtained transition points. Although the ground state energy of the system decreases after the occurrence of conventional and unconventional SPTs, it should be pointed out that they do not belong to the same phase transition type. As shown in Fig. 1(c), the second-order derivative of $\text{Re}(E_0)/\eta$ under $\phi = \frac{\pi}{2}$ and $g = 0.7$ is not continuous at the transition point. Figure 1(d) shows that the first-order derivative of $\text{Re}(E_0)/\eta$ under $\phi = \frac{\pi}{4}$ and $g = 0.4$. The results show that the conventional SPT should be the second-order quantum phase transition, while the unconventional SPT should be the first-order quantum phase transition. In fact, only the $|\phi| = \frac{\pi}{4}$ and $|\phi| = \frac{3\pi}{4}$ cases correspond to the second-order quantum phase transition, while the cases with other ϕ correspond to the first-order quantum phase transition. However, we are more concerned with conventional and unconventional superradiance phase transitions in this paper, so the results of other ϕ are not considered.

Except for the ground-state energy, the phenomenon of SPT can be readily seen from the ground-state photon population. Under $\phi = \frac{\pi}{2}$, ground-state photon populations $\langle a_{1(2)}^\dagger a_{1(2)} \rangle$ for $g = 0.5$ and $g = 0.7$ are plotted in Fig. 3(a) and 3(b), respectively. It is seen that there is no photon excitation when \mathcal{J} is smaller than the transition point, but there are macroscopic photon excitations when the cavity coupling parameter \mathcal{J} exceeds the transition

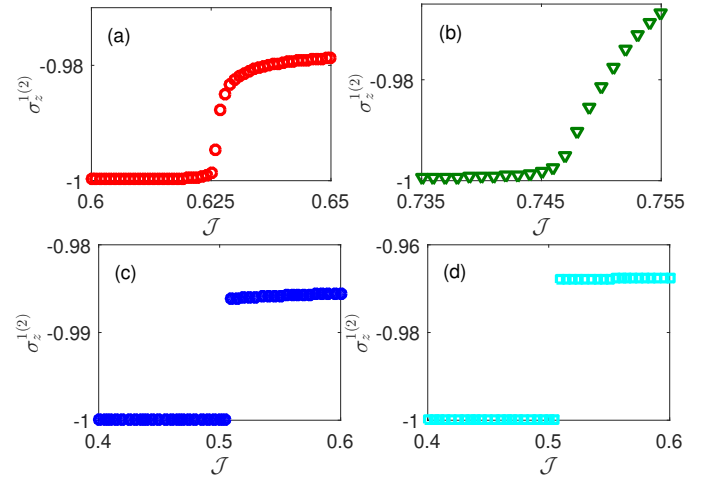


Figure 4. (Color online) The ground-state atom population $\sigma_z^{1(2)}$ as a function of \mathcal{J} . (a) $g = 0.5$ and $\phi = \frac{\pi}{2}$; (b) $g = 0.7$ and $\phi = \frac{\pi}{2}$; (c) $g = 0.4$ and $\phi = \frac{\pi}{4}$; (d) $g = 0.6$ and $\phi = \frac{\pi}{4}$. The photonic truncation number is $N = 80$ and $\eta = 1500$.

point. The phenomenon is similar to the $\phi = \frac{\pi}{4}$ case. For $g = 0.4$ and $g = 0.6$, the corresponding ground-state photon populations are plotted in Fig. 3(c) and 3(d), respectively. We can see that there are macroscopic photon excitations when \mathcal{J} is larger than 0.5 , while the photon excitations are evidently suppressed when $J < 0.5$.

A reasonable explanation for the macroscopic photon excitations in the superradiance phase is that the atoms are excited and become active. To check this point, the atom populations $\langle \sigma_z^{1(2)} \rangle$ as a function of \mathcal{J} for different ϕ and g are plotted in Fig. 4(a)-4(d). We can see that when \mathcal{J} is smaller than the transition point, the atoms are stable in the ground state, with populations $\langle \sigma_z^{1(2)} \rangle = -1$. When \mathcal{J} crosses the transition point, it is seen that the populations of atoms deviate from -1 , implying that the atoms are excited and become active. The excited atoms dominate the macroscopic photon excitations in the SPT. Although the photon excitations and the atom populations of the system vary obviously with occurrence of SPT, the two types of SPTs lead to different varying behaviors of observables. From Fig. 3, we can see that when the conventional SPT happens, $\langle a_{1(2)}^\dagger a_{1(2)} \rangle$ continuously varies to macroscopic value, while the unconventional SPT happens, $\langle a_{1(2)}^\dagger a_{1(2)} \rangle$ directly jumps to macroscopic values without asymptotic process. Similarly, we can see the obvious difference between the two types of SPTs from the atomic populations in Fig. 4.

In addition to the photon population and the atom population, the excitation gaps behind the two types of SPTs are different as well. The excitation gaps here contain two meanings. One is the real excitation gap $\text{Re}(\Delta_E)/\eta$ between the real parts of the lowest two energies. Another is the imaginary excitation gap $\text{Im}(\Delta_E)/\eta$ between the imaginary parts of the lowest two ener-

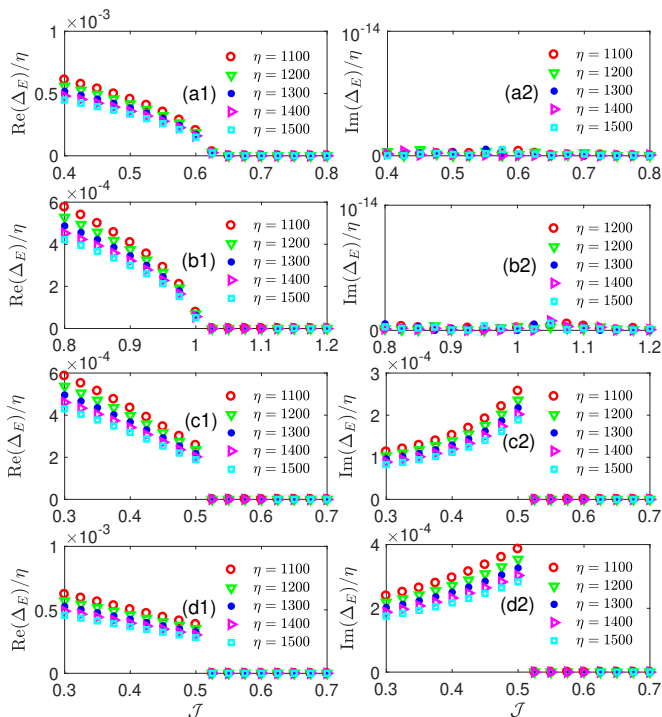


Figure 5. (Color online) The excitation gaps $\text{Re}(\Delta_E)$ and $\text{Im}(\Delta_E)$ as functions of \mathcal{J} under different η . (a1) and (a2): $g = 0.5$ and $\phi = \frac{\pi}{2}$; (b1) and (b2): $g = 1$ and $\phi = \frac{\pi}{2}$; (c1) and (c2): $g = 0.4$ and $\phi = \frac{\pi}{4}$; (d1) and (d2): $g = 0.6$ and $\phi = \frac{\pi}{4}$. The photonic truncation number is $N = 36$.

gies. Figures. 5(a1)-5(d1) (Figs. 5(a2)-5(d2)) presents $\text{Re}(\Delta_E)/\eta$ ($\text{Im}(\Delta_E)/\eta$) as a function of \mathcal{J} under different η . We can see that no matter $\phi = \frac{\pi}{2}$ and $\phi = \frac{\pi}{4}$, the real excitation gap experiences a gap closing process when \mathcal{J} exceeds the transition point. However, for the imaginary excitation gap, there is an obvious difference between the two studied cases. From Figs. 5(a2) and 5(b2), we can see that $\text{Im}(\Delta_E)/\eta$ always keeps zero ($\text{Im}(\Delta_E)/\eta$ far less than 10^{-14} can be numerically regarded as zero.) before and after the transition point. From Figs. 5(c2) and 5(d2), we can see that the imaginary excitation gaps experience the gap closing process, similar to the circumstances for the real excitation gaps.

It is noted that for a \mathcal{PT} -symmetric Rabi system, there exists real-complex transition in energy spectrum [40, 41, 43–45]. Surprisingly, for the non-Hermitian two-Rabi cavity system without \mathcal{PT} symmetry, there exists real energy spectrum as well. Under $\phi = \frac{\pi}{2}$, the maximal imaginary of the energy spectra for $g = 0.7$ and $g = 0.8$, i.e., $\text{Im}(E)_{max}$ are plotted in Figs. 6(a) and 6(b), respectively. The analytically obtained superradiance transition point for $g = 0.7$ is $J = 0.745$, and that for $g = 0.8$ is $J = 0.82$. $\text{Im}(E)_{max}/\eta$ approaches to zero before and after the superradiance transition point implying that the energy spectra under $\phi = \frac{\pi}{2}$ are real, and there is no real-complex transition in energy spectrum. Compared to the $\phi = \frac{\pi}{2}$ case, the spectral property of

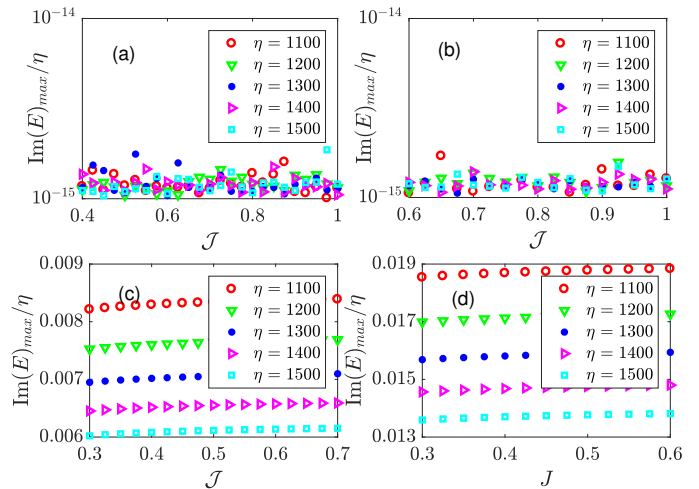


Figure 6. (Color online) The maximal imaginary part of the energy spectrum $\text{Im}(E)_{max}/\eta$ as functions of \mathcal{J} under different η . (a) $\phi = \frac{\pi}{2}$ and $g = 0.7$. (b) $\phi = \frac{\pi}{2}$ and $g = 0.8$. (c) $\phi = \frac{\pi}{4}$ and $g = 0.4$. (d) $\phi = \frac{\pi}{4}$ and $g = 0.6$. The photonic truncation number is $N = 36$.

the $\phi = \frac{\pi}{4}$ is different. Under $\phi = \frac{\pi}{4}$, $\text{Im}(E)_{max}/\eta$ for $g = 0.4$ and $g = 0.6$ are plotted in Figs. 6(c) and 6(d), respectively. Different from the $\phi = \frac{\pi}{2}$ cases, here the energy spectra are complex because of the nonvanishing $\text{Im}(E)_{max}/\eta$. In fact, the real and complex characteristics of the energy spectrum can be understood analytically as well. From Eq. (10) and Eq. (13), we know that when $\phi = \frac{\pi}{2}$, the imaginary part disappears, but when $\phi = \frac{\pi}{4}$, the imaginary part still exists. The results in Fig. 6 provide numerical validation of the previous analytical derivation. Considering the fact that the $\phi = \frac{\pi}{2}$ cases have full real energy spectra, we conjecture that here the conventional SPT belongs to the same universality class as the Hermitian Rabi systems [28, 30, 32–35] and the critical exponent of the phase transition can be obtained from the critical behavior. However, for the complex energy spectrum case ($\phi = \frac{\pi}{4}$), we conjecture that there is no critical behavior. Although the existence of quantum criticality of conventional SPT and the absence of quantum criticality of unconventional SPT have been reflected in the photon population and atom population, we still want to further verify them by studying the ground-state fidelity and fidelity susceptibility.

V. CONVENTIONAL AND UNCONVENTIONAL SUPERRADIANCE PHASE TRANSITION

We focus on the quantum phase transition and its critical behavior triggered by the cavity coupling parameter \mathcal{J} . The fidelity for the ground state \mathcal{F} is defined as [46–49]

$$\mathcal{F} = |\langle \psi_0(\mathcal{J}) | \psi_0(\mathcal{J} + \delta\mathcal{J}) \rangle|, \quad (14)$$

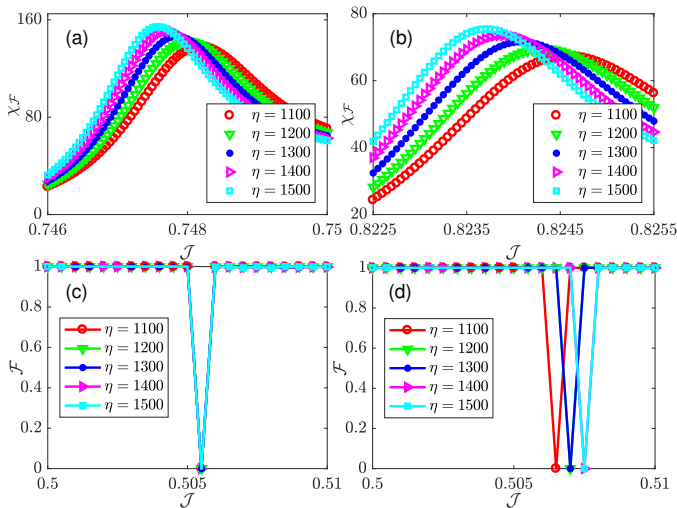


Figure 7. (Color online) Fidelity susceptibility $\chi_{\mathcal{F}}$ as functions of \mathcal{J} under different η with $\varphi = \frac{\pi}{2}$ and $g = 0.7$ in (a), and with $\varphi = \frac{\pi}{2}$ and $g = 0.8$ in (b). The involved parameter is $\delta\mathcal{J} = 10^{-5}$. Fidelity \mathcal{F} as functions of \mathcal{J} under different η with $\varphi = \frac{\pi}{4}$ and $g = 0.4$ in (c), and with $\varphi = \frac{\pi}{4}$ and $g = 0.6$ in (d). The involved parameter is $\delta\mathcal{J} = 5 \times 10^{-4}$. The photonic truncation number in all calculations is $N = 80$.

which weighs the survival probability of the ground state after the cavity coupling parameter \mathcal{J} from an infinitesimal distance $\delta\mathcal{J}$. Further, according to Refs. [50–54], we can obtain the fidelity susceptibility $\chi_{\mathcal{F}}$ as

$$\chi_{\mathcal{F}} = \lim_{\delta\mathcal{J} \rightarrow 0} \frac{-2 \ln \mathcal{F}(\mathcal{J}, \delta\mathcal{J})}{(\delta\mathcal{J})^2}. \quad (15)$$

If there exists quantum phase transition, the fidelity will experience a drop at the phase transition point, and the fidelity susceptibility will peak at the phase transition point.

Under $\varphi = \frac{\pi}{2}$, $\chi_{\mathcal{F}}/\eta$ for $g = 0.7$ and $g = 0.8$ are plotted in Figs. 7(a) and 7(b), respectively. As seen that with the increase of \mathcal{J} , $\chi_{\mathcal{F}}/\eta$ smoothly reaches the peak and then smoothly decreases. Besides, $\chi_{\mathcal{F}}/\eta$ presents obvious critical behaviors, because it is seen that with the increase of η , the peak of $\chi_{\mathcal{F}}$ at the coupling parameter \mathcal{J}_{max} gradually tends to the exact solution. Moreover, with the increase of η , the peak of $\chi_{\mathcal{F}}$ get higher. However, for the $\varphi = \frac{\pi}{4}$ cases, there is no critical phenomenon. Under $\varphi = \frac{\pi}{4}$, the fidelity \mathcal{F} for $g = 0.4$ and $g = 0.6$ are plotted in Figs. 7(c) and 7(d), respectively. Intuitively, \mathcal{F} sharply drop to zero at single parameter \mathcal{J} and there is no asymptotic behavior between the valley of \mathcal{F} (or the peak of $\chi_{\mathcal{F}}$) and η . In other words, the conventional SPT exists quantum criticality while there is no quantum criticality for the unconventional SPT.

Next, we study the quantum criticality of the conventional SPT ($\varphi = \frac{\pi}{2}$ case). From the $\chi_{\mathcal{F}}-\eta$ curves, the maximal fidelity susceptibility $\chi_{\mathcal{F}}^{max}$ under a specific η is obtained. Then, the universal finite η scaling relation of $\chi_{\mathcal{F}}$ for $g = 0.7$ is plotted in Fig. 8(a). The black fitting

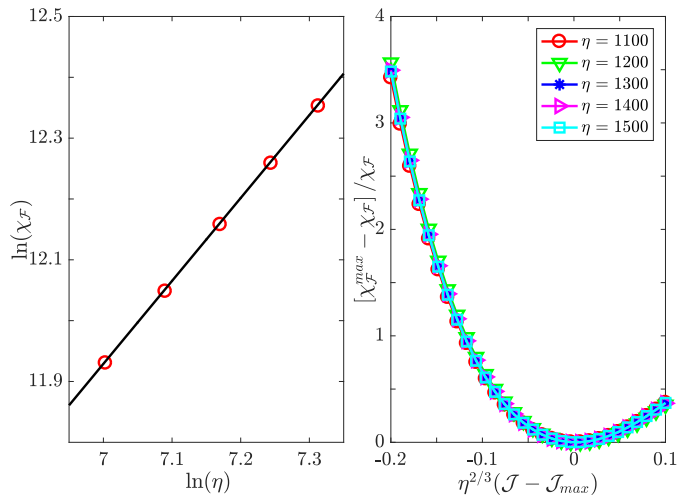


Figure 8. (Color online) (a) Universal finite η scaling relation of the maximal fidelity susceptibility $\chi_{\mathcal{F}}^{max}$. (b) Data collapse of $[\chi_{\mathcal{F}}^{max} - \chi_{\mathcal{F}}]/\chi_{\mathcal{F}}$. The involved parameters are $\varphi = \frac{\pi}{2}$, $g = 0.7$, and $\delta\mathcal{J} = 10^{-5}$.

curve satisfies $\ln \chi_{\mathcal{F}} = (-1.363 \pm 0.004) \ln \eta + 2.388$. It implies the scaling exponent μ of $\chi_{\mathcal{F}}$ is $\mu = -1.363 \pm 0.004$. As introduced in Ref. [32, 55], the relationship between μ and ν obeys $\mu = \frac{2}{\nu}$, by which we obtain $\nu = 1.4674 \pm 0.004$. Although the numerically obtained critical exponents μ and ν has slightly numerical deviation from the exact solution (with $\nu_{exact} = 3/2$) of the single Rabi model [28, 30], we argue that the quantum phase transition in the $\varphi = \frac{\pi}{2}$ is the same universality class as that in the single Rabi model. Within the neighborhood of the phase transition point, $\chi_{\mathcal{F}}$ scales as $[\chi_{\mathcal{F}}^{max} - \chi_{\mathcal{F}}]/\chi_{\mathcal{F}} = f[\eta^{1/\nu}(\mathcal{J} - \mathcal{J}_{max})]$, where $f(x)$ is a universal scaling function. Under different η , we find the corresponding data of $[\chi_{\mathcal{F}}^{max} - \chi_{\mathcal{F}}]/\chi_{\mathcal{F}}$ are collapsed into one curve with the exact critical exponent $\nu = \frac{3}{2}$, signaling the same universality class as the single Rabi model [28, 30]. In fact, for the Dicke model [56, 57] and the Lipkin-Meshkov-Glick model [58–60], the critical exponent satisfies $3/2$ as well, therefore the conventional SPT of the non-Hermitian cascade Rabi cavities we have studied belongs to the same universality class as those in the above mentioned systems.

VI. EXPERIMENTAL FEASIBILITY

The experimental exploration of the phenomena discussed here could be facilitated by a proposed circuit-QED architecture, as detailed in Ref. [61]. This setup comprises two resonators, each equipped with an embedded artificial atom, specifically a superconducting flux qubit. The key feature of this design is the implementation of a coupling mechanism between the resonators that is both broadly and rapidly tunable. By leveraging fast-modulating fields, this tunable coupling can ef-

fectively emulate a phase-dependent interaction term, a crucial component for investigating PT-related physics. Furthermore, the architecture allows for the coupling between the flux qubits and the resonators to be pushed into the ultrastrong coupling regime ($g > 0.1$), and even the deep-strong coupling regime ($g > 1$). These advanced capabilities of the circuit-QED system provide a solid platform not only for testing the theoretical predictions presented in this article but also for realizing these concepts in practical, soon-to-be-available devices.

VII. SUMMARY

Herein, a non-Hermitian QRM consisting of two cascaded non-Hermitian Rabi cavities has been studied. Similar to Hermitian QRMs, the superradiance phase boundary of the non-Hermitian one can be exactly solved as well. Accompanied by the emergence of SPT, the ground state energy gets lower. Meanwhile, the atoms become active and radiating photons outward. However, the non-Hermiticity leads to the exotic phenomena without Hermitian counterpart. When the atom-optical field coupling phase satisfies $\varphi = \pm \frac{\pi}{4}$ or $\varphi = \pm \frac{3\pi}{4}$, the superradiance phase boundary is surprisingly dominated by a

constant independent of the strength of the atom-cavity field coupling, suggesting the unconventional SPT. For other coupling phases, the superradiance phase boundary depends on the cavity coupling strength and the atom-optical field coupling strength together, suggesting the conventional SPT. Meanwhile, we have argued that the conventional SPT belongs to the second-order quantum phase transition, while the unconventional SPT belongs to the first-order quantum phase transition. Even though the model we have studied is not \mathcal{PT} -symmetric, there still exists fully real energy spectrum. By the photon population, atom population, and the fidelity we have known that there is no quantum criticality for the unconventional SPT due to characteristics of the absence of asymptotic process and the single-parameter sharp drop of fidelity. Differently, for conventional SPT, there exists quantum criticality, and the critical exponent extracted from the scaling analyze of fidelity susceptibility show that the SPT belong to the same universality class as the single Rabi model. With the development of circuit-QED experimental technique, the found SPTs may be realized in high-performance circuit-QED architecture.

We acknowledge the support from NSFC under Grant No. 12174346.

-
- [1] I. I. Rabi, On the Process of Space Quantization, *Phys. Rev.* **49**, 324 (1936).
- [2] P. Meystre, *Quantum Optics, Graduate Texts in Physics* (Springer, Cham, 2021).
- [3] R. H. Dicke, Coherence in spontaneous radiation processes, *Phys. Rev.* **93**, 99 (1954).
- [4] M. Kus and M. Lewenstein, Exact isolated solutions for the class of quantum optical systems, *J. Phys. A* **19**, 305 (1986).
- [5] C. Emary and R. F. Bishop, Bogoliubov transformations and exact isolated solutions for simple nonadiabatic Hamiltonians, *J. M. Phys.* **43**, 3916 (2002).
- [6] I. D. Feranchuk, L. I. Komarov, and A. P. Ulyanenko, Two-level system in a one-mode quantum field: numerical solution on the basis of the operator method, *J. Phys. A* **29**, 4035 (1996).
- [7] E. K. Irish, Generalized Rotating-Wave Approximation for Arbitrarily Large Coupling, *Phys. Rev. Lett.* **99**, 173601 (2007).
- [8] S. Ashhab and F. Nori, Qubit-oscillator systems in the ultrastrong, *Phys. Rev. A* **81**, 042311 (2010).
- [9] C. J. Gan and H. Zheng, Dynamics of a two-level system coupled to a quantum oscillator: transformed rotating-wave approximation, *Eur. Phys. J. D* **59**, 473 (2010).
- [10] J. Hausinger and M. Grifoni, Qubit-oscillator system: An analytical treatment of the ultra-strong coupling regime, *Phys. Rev. A* **82**, 062320 (2011).
- [11] V. V. Albert, G. D. Scholes and P. Brumer, Symmetric rotating-wave approximation for the generalized single-mode spin-boson system, *Phys. Rev. A* **84**, 042110 (2011).
- [12] V. Bargmann, On a Hilbert space of analytic functions and an associated integral transform, *Comm. Pure Appl. Math.* **14**, 187 (1961).
- [13] D. Braak, Integrability of the Rabi Model, *Phys. Rev. Lett.* **107**, 100401 (2011).
- [14] Q. H. Chen, C. Wang, S. He, T. Liu, and K. L. Wang, Exact solvability of the quantum Rabi model using Bogoliubov operators, *Phys. Rev. A* **86**, 023822 (2012).
- [15] L. W. Duan, S. He, D. Braak, Q.-H. Chen, Solution of the two-mode quantum Rabi model using extended squeezed states, *Euro. Phys. Lett.* **112**, 34003 (2015).
- [16] L. W. Duan, Y.-F. Xie, D. Braak, Q.-H. Chen, Two-photon Rabi model: analytic solutions and spectral collapse, *J. Phys. A* **49**, 464002 (2016).
- [17] D. Braak, Q.-H. Chen, M. T. Batchelor and E. Solano, Semi-classical and quantum Rabi models, *J. Phys. A* **49**, 300301 (2016).
- [18] Q.-T. Xie, H.-H. Zhong, M. T. Batchelor, and C.-H. Lee, The quantum Rabi model: solution and dynamics, *J. Phys. A* **50**, 113001 (2017).
- [19] P. Forn-Díaz, L. Lamata, E. Rico, J. Kono, E. Solano, Ultrastrong coupling regimes of light-matter interaction, *Rev. Mod. Phys.* **91**, 025005 (2019).
- [20] M. S. Choi, Exotic Quantum States of Circuit Quantum Electrodynamics in the Ultra-Strong Coupling Regime, *Adv. Quantum Technol.* 2000085 (2020)
- [21] J. Li and Q.-H. Chen, Two-photon Rabi-Stark model, *J. Phys. A: Math. Theor.* **53**, 315301 (2020).
- [22] Y.-F. Xie and Q.-H. Chen, Double degeneracy associated with hidden symmetries in the asymmetric two-photon Rabi model, *Phys. Rev. Research* **3**, 033057 (2021).
- [23] Y.-F. Xie and Q.-H. Chen, Two-photon Rabi model: analytic solutions and spectral collapse, *J. Phys. A: Math.*

- Theor. **55**, 425204 (2022).
- [24] D. Braak, Spectral Determinant of the Two-Photon Quantum Rabi model, *Ann. Phys. (Berlin)* **535**, 2200519 (2023).
- [25] R. Grimaudo, A. S. Magalhães de Castro, A. Messina, E. Solano, and D. Valenti, Quantum Phase Transitions for an Integrable Quantum Rabi-like Model with two Interacting Qubits, *Phys. Rev. Lett.* **130**, 043602 (2023).
- [26] Z.-J. Ying, From Quantum Rabi Model To Jaynes–Cummings Model: Symmetry-Breaking Quantum Phase Transitions, Symmetry-Protected Topological Transitions and Multicriticality, *Adv. Quantum Technol.* **5**, 2270013 (2022).
- [27] Z.-J. Ying, Spin Winding and Topological Nature of Transitions in Jaynes-Cummings Model with Stark Nonlinear Coupling, *Phys. Rev. A* **109**, 053705 (2024).
- [28] M.-J. Hwang, R. Puebla, and M. B. Plenio, Quantum Phase Transition and Universal Dynamics in the Rabi Model, *Phys. Rev. Lett.* **115**, 180404 (2015).
- [29] M.-J. Hwang and M. B. Plenio, Quantum Phase Transition in the Finite Jaynes-Cummings Lattice Systems, *Phys. Rev. Lett.* **117**, 123602 (2016).
- [30] M. X. Liu, S. Chesi, Z.-J. Ying, X. S. Chen, H.-G. Luo, and H.-Q. Lin, Universal Scaling and Critical Exponents of the Anisotropic Quantum Rabi Model, *Phys. Rev. Lett.* **119**, 220601 (2017).
- [31] M.-J. Hwang, M. S. Kim, and M.-S. Choi, Recurrent Delocalization and Quasiequilibration of Photons in Coupled Systems in Circuit Quantum Electrodynamics, *Phys. Rev. Lett.* **116**, 153601 (2016).
- [32] B.-B. Wei and X.-C. Lv, Fidelity susceptibility in the quantum Rabi model, *Phys. Rev. A* **97**, 013845 (2018).
- [33] Y. Ming, M. Liu, W.-L. You, S. Chesi, H.-G. Luo, and H.-Q. Lin, Resilience of the superradiant phase against A^2 effects in the quantum Rabi dimer, *Phys. Rev. A* **106**, 063843 (2020).
- [34] B.-B. Mao, L. Li, W.-L. You, and M. Liu, Superradiant phase transition in quantum Rabi dimer with staggered couplings, *Physica A* **564**, 125534 (2021).
- [35] Y.-Y. Zhang, Z.-X. Hu, L. Fu, H.-G. Luo, H. Pu, and X.-F. Zhang, Quantum Phases in a Quantum Rabi Triangle, *Phys. Rev. Lett.* **127**, 063602 (2021).
- [36] D. F. Padilla, H. Pu, G.-J. Cheng, and Y.-Y. Zhang, Understanding the quantum Rabi ring using analogies to quantum magnetism, *Phys. Rev. Lett.* **129**, 183602 (2022).
- [37] Y.-Q. Lu and Y.-Y. Zhang, Quantum tricriticality and universal scaling in a tricritical quantum Rabi system, arXiv: 2402.12827 (2024).
- [38] Y. Cao and J. Cao, Exact Solution of a Non-Hermitian Generalized Rabi Model, *Chin. Phys. Lett.* **38**, 080202 (2021).
- [39] T. E. Lee and Y. N. Joglekar, \mathcal{PT} -symmetric Rabi model: Perturbation theory, *Phys. Rev. A* **92**, 042103 (2015).
- [40] C. M. Bender and S. Boettcher, Real Spectra in Non-Hermitian Hamiltonians Having \mathcal{PT} Symmetry, *Phys. Rev. Lett.* **80**, 5243 (1998).
- [41] B. Zhu, R. Lü, and S. Chen, \mathcal{PT} symmetry in the non-Hermitian Su-Schrieffer-Heeger model with complex boundary potentials, *Phys. Rev. A* **89**, 062102 (2014).
- [42] W. D. Heiss, The physics of exceptional points, *J. Phys. A: Math. Theor.* **45**, 444016 (2012).
- [43] Q. Xie, S. Rong, and X. Liu, Exceptional points in a time-periodic parity-time-symmetric Rabi model, *Phys. Rev. A* **98**, 052122 (2018).
- [44] X. Lu, H. Li, J.-K. Shi, L. B. Fan, V. Mangazeev, Z.-M. Li, and M. T. Batchelor, \mathcal{PT} -symmetric quantum Rabi model, **108**, 053712 (2023).
- [45] L. Li, Y.-C. Wang, L.-W. Duan, and Q.-H. Chen, The \mathcal{PT} -symmetric quantum Rabi model: Solutions and exceptional points, arXiv: 2402.09749.
- [46] M. A. Nilesen and I. L. Chuang, *Quantum Computation and Quantum Information* (Cambridge University Press, Cambridge, England, 2000).
- [47] H. T. Quan, Z. Song, X. F. Liu, P. Zanardi, and C. P. Sun, Decay of Loschmidt Echo Enhanced by Quantum Criticality, *Phys. Rev. Lett.* **96**, 140604 (2006).
- [48] P. Zanardi and N. Paunković, *Phys. Rev. E* **74**, 031123 (2006).
- [49] S. J. Gu, Fidelity approach to quantum phase transitions, *Int. J. Mod. Phys. B* **24**, 4371 (2010).
- [50] W.-L. You, Y.-W. Li, and S. J. Gu, Fidelity, dynamic structure factor, and susceptibility in critical phenomena, *Phys. Rev. E* **76**, 022101 (2007).
- [51] P. Zanardi, P. Giorda, and M. Cozzini, Information-Theoretic Differential Geometry of Quantum Phase Transitions, *Phys. Rev. Lett.* **99**, 100603 (2007).
- [52] L. Campos Venuti and P. Zanardi, *Phys. Rev. Lett.* **99**, 095701 (2007).
- [53] S.-J. Gu, H.-M. Kwok, W.-Q. Ning, and H.-Q. Lin, Fidelity susceptibility, scaling, and universality in quantum critical phenomena, *Phys. Rev. B* **77**, 245109 (2008).
- [54] A. F. Albuquerque, F. Alet, C. Sire, and S. Capponi, Quantum critical scaling of fidelity susceptibility, *Phys. Rev. B* **81**, 064418 (2010).
- [55] A. Polkovnikov, K. Sengupta, A. Silva, and M. Vengalattore, Colloquium: Nonequilibrium dynamics of closed interacting quantum systems, *Rev. Mod. Phys.* **83**, 863 (2011).
- [56] J. Vidal and S. Dusuel, Finite-size scaling exponents in the Dicke model, *Europhys. Lett.* **77**, 817 (2006).
- [57] Tao Liu, Yu-Yu Zhang, Qing-Hu Chen, and Ke-Lin Wang, Large- N scaling behavior of the ground-state energy, fidelity, and the order parameter in the Dicke model, *Phys. Rev. A* **80**, 023810 (2009).
- [58] S. Dusuel and J. Vidal, Finite-Size Scaling Exponents of the Lipkin-Meshkov-Glick Model, *Phys. Rev. Lett.* **93**, 237204 (2004).
- [59] S. Dusuel and J. Vidal, Continuous unitary transformations and finite-size scaling exponents in the Lipkin-Meshkov-Glick model, *Phys. Rev. B* **71**, 224420 (2005).
- [60] H.-M. Kwok, W.-Q. Ning, S.-J. Gu, and H.-Q. Lin, Quantum criticality of the Lipkin-Meshkov-Glick model in terms of fidelity susceptibility, *Phys. Rev. E* **78**, 032103 (2008).
- [61] F. Quijandría, U. Naether, S. K. Özdemir, F. Nori, and D. Zueco, \mathcal{PT} -symmetric circuit QED, *Phys. Rev. A* **97**, 053846 (2018).